nature structural & molecular biology

Structure of the mammalian 80S initiation complex with initiation factor 5B on HCV-IRES RNA

Hiroshi Yamamoto[1,3], Anett Unbehaun[1,3], Justus Loerke[1], Elmar Behrmann[1], Marianne Collier[1], Jörg Bürger[1,2], Thorsten Mielke[1,2] & Christian M T Spahn[1]

The universally conserved eukaryotic initiation factor (eIF) 5B, a translational GTPase, is essential for canonical translation initiation. It is also required for initiation facilitated by the internal ribosomal entry site (IRES) of hepatitis C virus (HCV) RNA. eIF5B promotes joining of 60S ribosomal subunits to 40S ribosomal subunits bound by initiator tRNA (Met-tRNA$_i^{Met}$). However, the exact molecular mechanism by which eIF5B acts has not been established. Here we present cryo-EM reconstructions of the mammalian 80S–HCV-IRES–Met-tRNA$_i^{Met}$–eIF5B–GMPPNP complex. We obtained two substates distinguished by the rotational state of the ribosomal subunits and the configuration of initiator tRNA in the peptidyl (P) site. Accordingly, a combination of conformational changes in the 80S ribosome and in initiator tRNA facilitates binding of the Met-tRNA$_i^{Met}$ to the 60S P site and redefines the role of eIF5B as a tRNA-reorientation factor.

Eukaryotic translation initiation is a highly regulated process within the translation cycle that proceeds via 48S and 80S initiation-complex intermediates. At least 12 eIFs facilitate recruitment of Met-tRNA$_i^{Met}$ and mRNA to the ribosomal 40S subunit and regulate the interaction of Met-tRNA$_i^{Met}$ with the translational machinery during scanning, initiation-codon selection and ribosomal subunit joining along the canonical 5′ end–dependent pathway of translation initiation[1]. In its last step, eIF5B, a translational GTPase, facilitates joining of the 60S subunit to the 48S complex assembled at the AUG codon of mRNA[2]. eIF5B is a general translation initiation factor required for optimum growth in yeast and for viability of mammalian cells and *Drosophila*[3–5]. It is an ortholog of bacterial initiation factor 2 (IF2), and it is one of the universally conserved initiation factors. Recently, eIF5B has been linked with ribosome maturation, during which it promotes 80S-like-complex assembly to check the quality of pre-40S particles devoid of mRNA and Met-tRNA$_i^{Met}$ (ref. 6).

Mammalian eIF5B is a 140-kDa protein consisting of a long, non-conserved N-terminal part (amino acids (aa) 1–628), a conserved core containing the G domain (aa 627–850), and a C terminus (aa 851–1220)[7]. The C-terminal half of eIF5B confers the ribosome-dependent GTPase and subunit-joining activity[2]. X-ray structures of archaeal aIF5B, naturally lacking the N terminus, have revealed a chalice-shaped molecule with a globular cup (domains I, II and III), a rigid 40-Å-long connecting stem (helix 12 of eIF5B) and a base (domain IV)[8]. Subunit joining occurs simultaneously with the release of initiation factors (eIF3 and eIF2–GDP) from the 40S and is mediated by the GTP-bound state of eIF5B[2,9,10]. In the newly assembled ribosome, hydrolysis of eIF5B–GTP is triggered by the 60S subunit, to allow the release of eIF5B–GDP to start translation elongation[2]. Moreover, GTP hydrolysis by eIF5B is required for stringent AUG-codon selection, stable ribosomal binding of Met-tRNA$_i^{Met}$ and elongation competence *in vivo*[11–13]. However, the molecular mechanism linking eIF5B–GTP hydrolysis and proper placement of Met-tRNA$_i^{Met}$ in the ribosomal P site is not known.

eIF5B is also one of the few factors required for most types of the alternative cap- and end-independent internal initiation[14–16] used by several viral RNAs. Internal initiation involves a reduced subset of initiation factors, and it is driven by specific *cis*-acting RNA-based structures in the 5′ untranslated region (UTR) called IRESes. IRESes are exemplified by the HCV-IRES and related HCV-type IRESes, such as the classical swine fever virus (CSFV) IRES[17]. The HCV-IRES initiation pathway starts with the high-affinity assembly of binary 40S–HCV-IRES complexes, which then bind Met-tRNA$_i^{Met}$–eIF2–GTP ternary complexes (eIF2-t.c.) to form the IRES analog of the 48S complex[18]. Alternatively, under conditions of low levels of eIF2-t.c., the HCV-IRES allows for eIF2-less assembly of 48S-like particles with Met-tRNA$_i^{Met}$, involving eIF5B and the multisubunit initiation factor eIF3. Such eIF2-less HCV-IRES–48S–like complexes readily associate with ribosomal 60S subunits, but IRES–48S analogs assembled with eIF2-t.c., like their canonical counterparts, require eIF5 for hydrolysis of eIF2–GTP and eIF5B for subunit assembly[16]. Hence, eIF5B acts on both the 48S and the 80S stage of the HCV-IRES initiation pathway.

Structural knowledge about the interaction of eIF5B with the 80S ribosome is crucial for a mechanistic understanding of the factor. In the bacterial system, intermediate-resolution cryo-EM maps of the interaction of IF2 with fMet-tRNA and 70S are available[19,20] (**Supplementary Note**). In eukaryotes, footprinting experiments have established initial models of the eIF5B-80S interaction[9,21] and recently, a cryo-EM reconstruction at 6.6-Å resolution of an

[1]Institute of Medical Physics and Biophysics, Charité–Universitätsmedizin, Berlin, Germany. [2]UltraStrukturNetzwerk, Max Planck Institute for Molecular Genetics, Berlin, Germany. [3]These authors contributed equally to this work. Correspondence should be addressed to C.M.T.S. (christian.spahn@charite.de).

Received 6 November 2013; accepted 20 June 2014; published online 27 July 2014; doi:10.1038/nsmb.2859

eIF5B-containing translation-initiation complex was published[22]. It provides insight into the interaction of eIF5B with the ribosome and initiator tRNA in the yeast system during canonical initiation.

To understand the role of eIF5B during HCV-IRES–facilitated internal initiation in the mammalian system, we have analyzed here the mammalian 80S–HCV-IRES–Met-tRNA$_i^{Met}$–eIF5B–5′-guanylyl imidodiphosphate (GMPPNP) complex by cryo-EM. Our study reveals not only overall similarities to the canonical yeast initiation complex but also unexpected differences. We obtained reconstructions of the mammalian complex in two substates including a new second state that was not observed for the bacterial and yeast complexes. The comparison of our structures suggests a model for eIF5B-mediated subunit joining in which eIF5B acts as a tRNA-reorientation factor.

RESULTS

Cryo-EM reconstruction of an 80S initiation complex

To provide structural insight into the action of eIF5B during subunit joining in the context of the HCV-IRES, we present here cryo-EM reconstructions of the mammalian 80S–HCV-IRES–Met-tRNA$_i^{Met}$–eIF5B–GMPPNP complex, which represents a common 80S intermediate along the eIF2- dependent and eIF2-independent initiation pathways on HCV-type IRESes[14–16]. We reconstituted the complex *in vitro* from 60S subunits and analogs of 48S HCV-IRES complexes lacking eIF2 (40S–HCV-IRES–Met-tRNA$_i^{Met}$–eIF5B–GMPPNP–eIF3)[14,15]. The small monomeric proteins eIF1 and eIF1A required for scanning and initiation-codon selection on 5′ end–dependent mRNAs were not included because they do not support, and can even inhibit, assembly of ribosomal complexes on HCV-type IRESes[14,18].

We analyzed the resulting complex by multiparticle cryo-EM to overcome sample heterogeneity[23]. We obtained cryo-EM maps of two subpopulations, both exhibiting density for the ligands HCV-IRES, eIF5B and one tRNA (**Fig. 1** and **Supplementary Fig. 1**). The two final maps reached resolutions of 8.9 Å and 9.5 Å with the classical 0.5 Fourier shell correlation (FSC) criteria (**Supplementary Fig. 2a**). Re-estimation of the resolution with a 'gold-standard' approach with 0.143 FSC criteria[24] resulted in even better nominal resolutions of 8.2 Å and 8.6 Å (**Supplementary Fig. 2b**). The subnanometer resolution enabled rigid-body fitting of the modeled rabbit eIF5B from crystal structures[8], with 33 additionally modeled N-terminal amino acids, and tRNA as well as cryo-EM models of the HCV-IRES RNA (M.C., H.Y. and C.M.T.S., unpublished data) and the human 80S ribosome[25]. No apparent density was present for eIF3, which is released during eIF5B-promoted subunit joining on 80S initiation complexes on cellular and HCV-IRES mRNAs[16,26,27].

Mammalian internal initiation uses subunit rolling

Interestingly, the two subpopulations of the mammalian 80S–HCV-IRES–Met-tRNA$_i^{Met}$–eIF5B–GMPPNP complex (**Fig. 2**) are distinguished by the rotational state of the ribosomal subunits, which in turn modifies the orientation of Met-tRNA$_i^{Met}$ in the P site and the interaction pattern of eIF5B with the ribosome (**Supplementary Table 1**). Surprisingly, the underlying conformational change in eIF5B-promoted subunit joining of HCV-IRES–driven internal initiation is not intersubunit rotation, which is well established for complexes of the bacterial ribosome with translational GTPases including the 70S–IF2–GMPPNP complex[19]. Eukaryotic initiation uses eukaryotic-specific subunit rolling, which we have recently identified by structural studies of mammalian translation-elongation complexes[25,28]. It corresponds to an approximately 6° orthogonal rotation around the long axis of the 40S subunit (**Fig. 2a**) and relates the post-translocational (Post) to the classical-1 pretranslocational (Pre) state of the mammalian 80S ribosome[25,28]. Because of this relation in terms of ribosome conformation, we will refer to the two subpopulations of the 80S–HCV-IRES–Met-tRNA$_i^{Met}$–eIF5B–GMPPNP complex as the Pre-like and the Post-like state, respectively. In addition, we observed local conformational changes on the 60S for the P and uL1 stalks (**Fig. 2b**). The P stalk is visible and in contact with domain I of eIF5B in the Pre-like state, but it appears disordered in the Post-like state (**Fig. 3a**,**b**). The uL1 stalk, which is visible in both complexes, is either more open or positioned toward the intersubunit side of the 60S in the Pre-and Post-like state, respectively.

Back-rolling results in a different state of tRNA

We compared the positions of initiator tRNA and eIF5B of the two substates in a common 40S-subunit alignment and found the ligands in overall similar positions (data not shown). In both substates, the anticodon stem of initiator tRNA is in the P site of the 40S, and the 3′-CCA end interacts with Arg1317 and Lys1357 and Lys1358 of domain IV of eIF5B, in agreement with functional data[29]. This interaction appears to be facilitated by a twist of the tRNA involving the acceptor stem and the 3′-CCA end (**Supplementary Fig. 3a**). The similarity of the ligand positions from the perspective of the 40S subunit means that the ligands largely follow the rolling movement of the 40S subunit and move relatively to the 60S subunit, to result in two

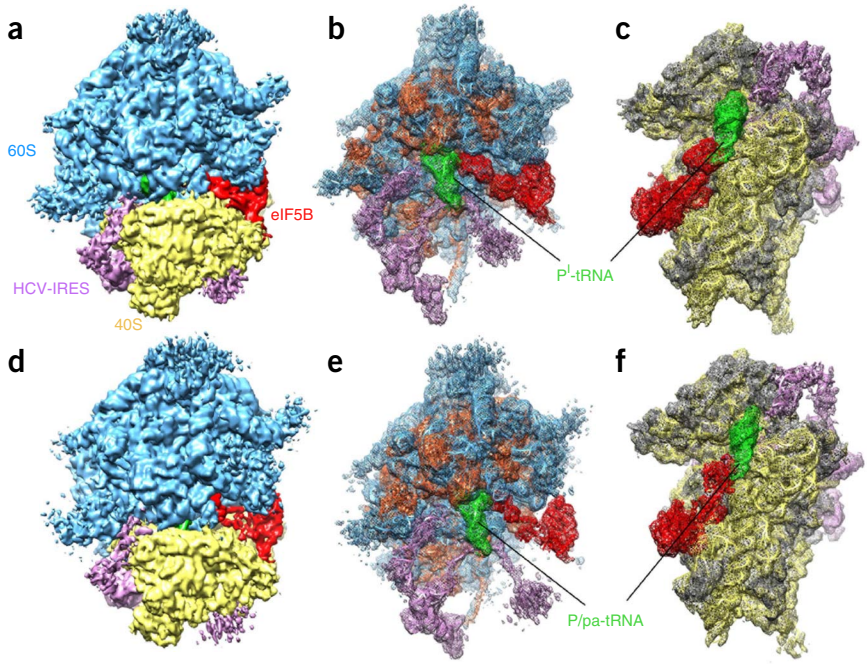

Figure 1 Cryo-EM reconstructions of the 80S–HCV-IRES–Met-tRNA$_i^{Met}$–eIF5B–GMPPNP complex. (**a**–**f**) Structures of substate I (Pre-like state) (**a**–**c**) and substate II (Post-like state) (**d**–**f**). (**a**,**d**) Overview of the structures with eIF5B (red), 40S subunit (yellow), 60S subunit (blue), HCV-IRES (purple), and tRNA (green). (**b**,**c**,**e**,**f**) Mesh representation of the map and docked models (colored as above) and 28S–5S–5.8S rRNA (blue), 60S proteins (orange), 18S rRNA (yellow) and 40S proteins (dark gray).

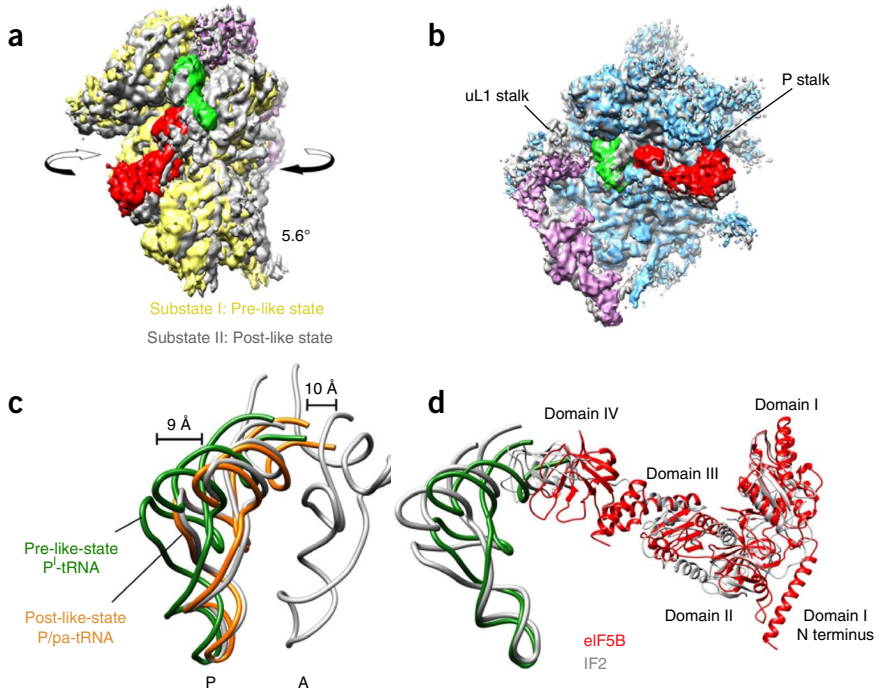

Figure 2 40S-subunit rolling rearranges initiator tRNA in the Pre- and Post-like states. (**a**,**b**) Comparison of the Pre-like state (colored as in **Fig. 1**) and the Post-like state (gray) in a common 60S alignment, in 40S view (**a**) and 60S view (**b**). The arrow in **a** indicates the back-rolling motion of the 40S between the Pre-like and Post-like states. (**c**) Configuration of the Pre-like-state P^I-tRNA (green) and the Post-like-state P/pa-tRNA (orange) from this study with classical A/A-tRNA and P/P-tRNA (gray) (PDB 3J0L)[25,28]. (**d**) Comparison of the Met-$tRNA_i^{Met}$–eIF5B–GMPPNP complex (colored as in **Fig. 1**) within the mammalian Pre-like state and the IF2–GMPPNP–fMet-$tRNA^{fMet}$ complex (gray) within the bacterial initiation complex (PDB 1ZO1)[19] in a common large-subunit alignment.

different ligand states. Accordingly, the P-site tRNA elbows are approximately 9 Å apart when the Pre-like and Post-like substates are compared from the perspective of the 60S subunit. In moving from the Pre-like state to the Post-like state, the tRNA elbow is positioned toward the P site. Owing to a conformational change in initiator tRNA, the movement of the CCA end appears even slightly larger (**Fig. 2c**).

The tRNA position in the present Pre-like state is to some extent reminiscent of the P/I state (with anticodon stem-loop at the P site and elbow and CCA end at the initiation position) of the fMet-tRNA in the bacterial 70S–IF2 complex[19] and thus represents the P^I configuration of eukaryotic initiator tRNA. Nevertheless, there are substantial differences in the positions of initiator tRNAs and IF2 (or eIF5B), because the tRNA body within the eukaryotic complex is placed closer to the P site than its bacterial counterpart (**Fig. 2d**). On a general level, the Pre-like state of our mammalian 80S–HCV-IRES–Met-$tRNA_i^{Met}$–eIF5B–GMPPNP complex corresponds well to the structure of the recently published canonical yeast initiation complex with eIF5B[22]. However, although both the mammalian Pre-like complex and the yeast complex contain initiator tRNA in P/I configuration in contact with eIF5B (**Supplementary Fig. 3b**), both models exhibit subtle differences in the exact positions of tRNA and domain IV of eIF5B (**Supplementary Fig. 3c**). In comparison to the yeast complex, in the mammalian complex the acceptor stem of Met-$tRNA_i^{Met}$ and domain IV of eIF5B reach deeper into the aminoacyl (A) site. Moreover, the CCA end of Met-$tRNA_i^{Met}$ has been modeled to interact with domain IV of eIF5B in the mammalian complex (but not in the yeast complex), in which it contacts helix H80 on 28S rRNA. We note that the cryo-EM density in this region is somehow less well defined than in the majority of the map, indicating potential residual flexibility. Thus, higher resolution will be required to address this issue.

The Post-like state of the present mammalian 80S–HCV-IRES–Met-$tRNA_i^{Met}$–eIF5B–GMPPNP complex has not been previously reported. As a result of subunit reverse rolling from the Pre-like to the Post-like ribosomal subunit configuration, the tRNA of the Post-like 80S–HCV-IRES–Met-$tRNA_i^{Met}$–eIF5B–GMPPNP complex is present in a previously unseen state with the tRNA elbow and the 3′-CCA end located in the P- and A-site regions of the 60S, respectively (**Fig. 2c**). After our previous

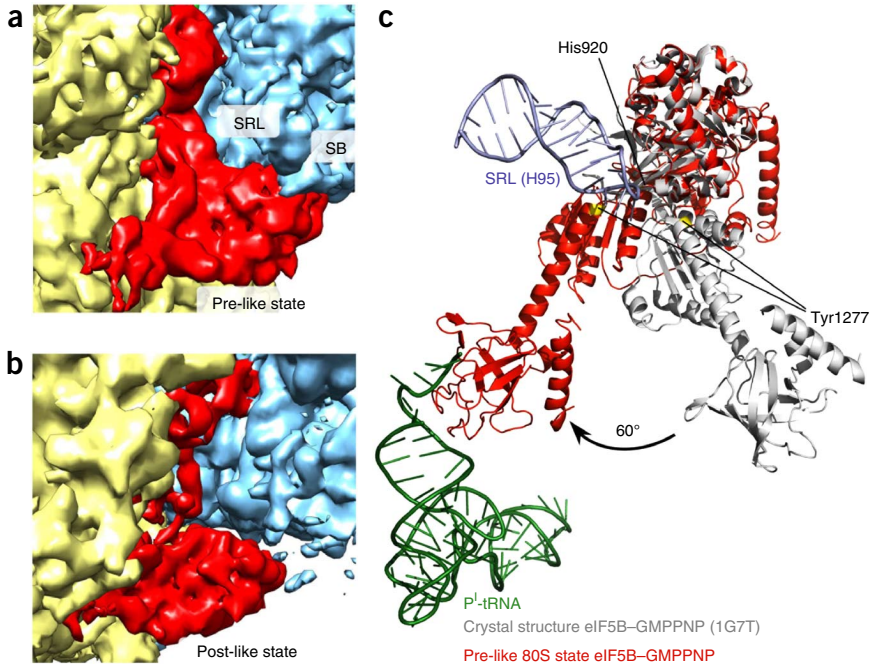

Figure 3 Interaction of eIF5B with the ribosome in the Pre- and Post-like states. (**a**,**b**) Contact of eIF5B with the stalk base (SB) and the sarcin-ricin loop (SRL) in the Pre-like and Post-like complex. Red, eIF5B; blue, 60S subunit; yellow, 40S subunit. (**c**) Superposition of domains I of isolated eIF5B (gray, PDB 1G7T)[8] and eIF5B (red) of the Pre-like complex, revealing movement of eIF5B domains III and IV (indicated with arrow) upon binding to the ribosome. Blue, SRL; green, P^I-tRNA.

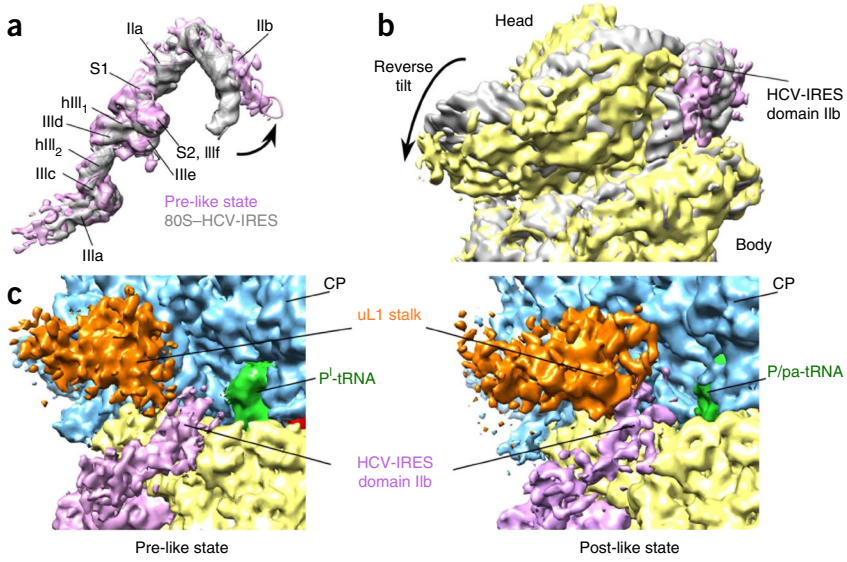

Figure 4 Movement of HCV-IRES domain II. (**a**) Comparison of HCV-IRES domain II in the Pre-like state (purple map and model) and the binary 80S–HCV-IRES complex (M.C., H.Y. and C.M.T.S., unpublished data; gray map and model) in a common 40S alignment. The arrow indicates the dynamics of the IRES domain II apex. (**b**) Comparison of the 40S–HCV-IRES domain II interaction in the binary 80S–HCV-IRES (gray) and Pre-like (colored) complex. The arrow indicates the reverse-tilt movement of the head domain of the 40S in the Pre-like complex. (**c**) The Pre-like state at low contour level with the tentative, transient interaction between HCV-IRES domain II (purple) and the elbow of P^I-tRNA (green). Yellow, 40S; blue, 60S with central protuberance (CP); orange, uL1-stalk.

nomenclature for intrasubunit hybrid states of tRNA[30], we denoted this chimeric configuration of tRNA the P/pa state (anticodon stem-loop at P site, elbow at P site and 3′-CCA end at A site). Because subunit rolling was not previously reported for the yeast initiation complex[22], this may indicate a specific distinction of the mammalian system or to HCV-IRES–facilitated internal initiation. However, there is a high degree of sequence conservation (overall 44%) between mammalian and yeast eIF5B, and accordingly human $eIF5B_{587–1220}$ can substitute yeast eIF5B in *in vitro* translation assays. We note that in a previous study the human factor only partially rescued a slow-growth phenotype of a yeast strain lacking eIF5B[11].

Interactions of eIF5B with the 40S and 60S subunits

The Pre-like and Post-like states of the 80S–HCV-IRES–Met-$tRNA_i^{Met}$–eIF5B–GMPPNP complex are distinguished by the interaction pattern of eIF5B with the ribosome. In the Pre-like complex, eIF5B is engaged in several contacts with both ribosomal subunits, which comply well with the known function of the protein as a subunit-joining factor (**Supplementary Table 1**). The N terminus, and in particular domain II, occupy a large interaction surface with the shoulder of the 40S, while domains I and III of eIF5B contact both subunits. The G domain of eIF5B–GMPPNP is positioned on the sarcin-ricin loop (SRL; helix (H) 95 of 28S rRNA), and an arc-like connection to the stalk base (SB; H43 and H44), via the P proteins of the 60S, is formed in a similar manner to that of the 80S–eEF2–GMPPNP complex[31] (**Fig. 3a**,**b** and **Supplementary Fig. 4a**,**b**). Owing to an approximately 60° rotation of domain III and IV of eIF5B between the isolated crystal structure[8] and the ribosome-bound structure, the Tyr1277 region of helix 12 in domain III interacts with the SRL (**Fig. 3c** and **Supplementary Fig. 4c**,**d**). Recent crystal structures of isolated eIF5B in apo, GDP-bound and GTP-bound states indicate that such positioning of domain III seems possible in the GTP-bound state of eIF5B only when domain III is released from its interaction with domain I[32].

These interactions of eIF5B domains I and III with the GTPase-associated center (GAC) suggest that GTP hydrolysis can be triggered in the Pre-like state. In the Post-like state, the G domain no longer contacts the 60S but still touches the 40S ribosome (**Supplementary Fig. 4e**,**f**), and the extensive interactions of domain II as well as the contacts between domain III and the N terminus with the small subunit remain intact. Domain IV of eIF5B does not touch the 40S subunit but interacts with domain V of the 28S rRNA in both states. Although both interaction partners provide the same contact sites in the Pre- and the Post-like states, their orientation with respect to each other is different (**Supplementary Fig. 4g**,**h**). In the Post-like state, we observed an additional interaction with the A loop, which binds the CCA end of A-site tRNA during elongation.

Dynamic movement of IRES domain II during initiation

The functional core of the HCV-IRES consists of hairpin domains II and IV and the branched hairpin domain III with the pseudoknot at the base[17]. In agreement with previous cryo-EM structures of the ribosome-bound IRES (ref. 33 and M.C., H.Y. and C.M.T.S., unpublished data), individual IRES domains and subdomains can be assigned in our structure (**Fig. 4a**). Comparison of the present 80S–HCV-IRES–Met-$tRNA_i^{Met}$–eIF5B–GMPPNP complexes to the binary 40S–HCV-IRES complex assembled without initiation factors reveals striking differences in the conformation of HCV-IRES domain II and its position

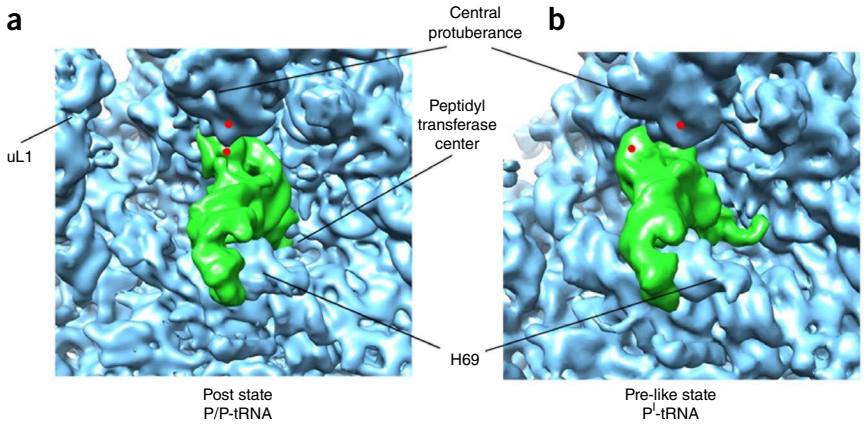

Figure 5 Subunit joining requires adjustment of initiator tRNA in the peptidyl transferase cleft of the 60S between the central protuberance and the H69 rim. (**a**,**b**) The isolated map of the 60S subunit and tRNA in a common 60S alignment for the Post state (EMD-2626)[25] (**a**) and Pre-like state (**b**). Red dots mark the elbow of tRNA and the central protuberance.

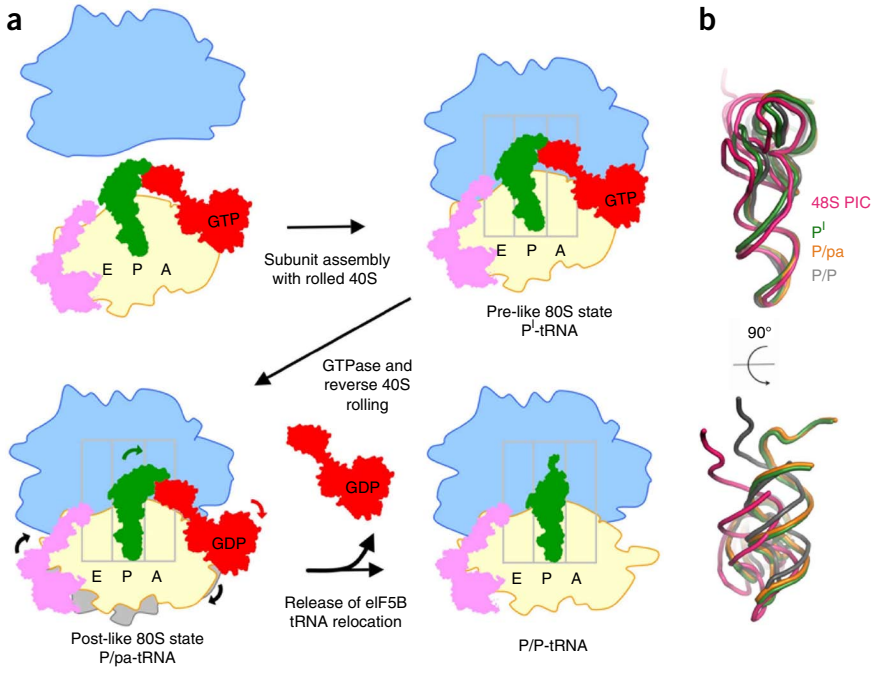

Figure 6 The trajectory of initiator tRNA suggests a model in which eIF5B acts as a tRNA-reorientation factor in ribosomal subunit joining. (**a**) eIF5B-promoted subunit joining to a 40S subunit (yellow) occurs with rolling and results in a Pre-like 80S initiation complex on the HCV-IRES (purple). eIF5B (red) and IRES domain II interact with Met-tRNA$_i^{Met}$ (green) and stabilize the P^I-tRNA configuration of the Pre-like state. Hydrolysis of eIF5B–GTP is triggered in the Pre-like state. Reverse rolling of the 40S establishes a P/pa-tRNA configuration and the Post-like state of the 80S initiation complex, in which the G domain of eIF5B is already displaced from the 60S subunit (blue). After dissociation of eIF5B–GDP from the Post-like state, the CCA end of the P/pa-tRNA is released from the A site into the final elongation-competent P/P-tRNA configuration. A, P and exit (E) sites are labeled. (**b**) Comparison of the positions of tRNA in the 48S PIC (pink, PDB 4KZZ)[43], P/P-tRNA of the Post state (gray) (PDB 4CXB)[25], P^I-tRNA (orange) and P/pa-tRNA (green) of the Pre- and Post-like states, respectively, in a common 40S alignment.

on the 40S subunit (**Fig. 4a**). The 40S head tilt is reversed, and the apical part of IRES subdomain IIb is released from its binding site on the 40S head (**Fig. 4b**).

This corroborates a dynamic interplay between IRES domain II and the 40S head during HCV-IRES–driven initiation. The density corresponding to IRES domain II appears fragmented, which is an indication of local heterogeneity due to flexibility of domain II. However, in the Pre-like complex, density attributable to the tip of IRES domain II approaches the elbow of P^I-tRNA at low contour level (**Fig. 4c**). In the Post-like complex, IRES domain II instead touches an inward-oriented L1 stalk (**Fig. 4c**). According to intensive biochemical studies, domain II (which disturbs ribosomal subunit joining with binary 40S–IRES complexes) is critically required for efficient 80S assembly on IRES–48S-like complexes because it affects eIF5-induced hydrolysis of eIF2–GTP and release of eIF2–GDP during subunit joining on the HCV and the related CSFV-IRES RNAs. Most importantly, IRES domain II was shown to be involved in the adjustment of Met-tRNA$_i^{Met}$ and the transition into elongation[14,16,34]. Hence, these functional data support a tentative and probably transient interaction of the IRES domain II apex with Met-tRNA$_i^{Met}$ in the Pre-like complex.

DISCUSSION

Cryo-EM maps rationalize previous functional data

Here, we have directly visualized GMPPNP-stalled eIF5B on mammalian 80S–HCV-IRES–Met-tRNA$_i^{Met}$ complexes to provide structural insight into ribosomal subunit joining in the context of internal initiation. eIF5B is bound to the general factor–binding site of translational GTPase factors, in excellent agreement with previous hydroxyl-radical probing studies[9,21] and an independent cryo-EM structure of a canonical yeast initiation complex[22]. Our structural study rationalizes previous mutational studies of yeast and mammalian eIF5B proteins with impaired function. The His920 residue of rabbit eIF5B (His706 in humans and His480 in yeast eIF5B) in the switch II loop of eIF5B's G domain is highly conserved among GTP-binding proteins[35]. In our Pre-like complex, His920 of eIF5B is placed in proximity of the SRL of 28S rRNA and the γ-phosphate of GTP, thus resembling the specific interaction of the corresponding histidine of EF-Tu with the large subunit to activate GTP hydrolysis[36]. Accordingly, mutations of this position destroy eIF5B function *in vivo* and *in vitro*[11–13].

As seen in other translational GTPases[37,38] as well, the switch I region of eIF5B contacts helix (h) 14 of 18S rRNA. This region is disordered in the isolated crystal structure of aIF5B[8] but is ordered in the ribosome-bound factor. Because the contact between h14 and the switch I region of eIF5B is maintained in both the Pre- and Post-like states (**Supplementary Fig. 4e**,**f**), it might stabilize the G domain even during the GTPase event. Consistently with this, the T870A mutation (T439A in yeast) in the switch I region yields a GTPase- and translation-deficient factor[13]. For both mutations in the switch I and II loop, suppressor mutants could be identified that restore subunit joining, factor release and general translation *in vitro* without restoring GTPase activity of eIF5B[13,21]. However, as reported for the T439A mutant, the lack of GTP hydrolysis by eIF5B impairs stable binding of Met-tRNA$_i^{Met}$ (ref. 13). Our structures suggest that the defect in switch I or switch II (like the nonhydrolyzable GTP analog of our complex) might stall eIF5B and that the suppressor mutant allows release of eIF5B after subunit assembly, but without proper guidance of tRNA from the P^I state via the P/pa state to the final P/P state.

Domain IV of eIF5B simultaneously contacts the P/pa tRNA and the A loop (H92) of the 60S subunit (**Supplementary Table 1**) in the Post-like complex. Recently, a mutational study in yeast reported such a functional interaction network of eIF5B to ensure stable subunit assembly and stringent AUG selection *in vivo*[39]. Our structural findings together with the yeast mutations indicate that domain IV of eIF5B might stabilize Met-RNA$_i^{Met}$ at the P site during transition from the P^I to the P/pa state and suggest that subunit reverse rolling (resulting in the described eIF5B-bridged interaction of the A loop with tRNA in P/pa tRNA configuration) is necessary for proper AUG selection before the final P/P state is reached. The aforementioned yeast study also indicates that the Post-like state with the P/pa tRNA configuration may be important not only for HCV-IRES–driven internal initiation but also for canonical initiation.

eIF5B acts as a reorientation factor for initiator tRNA

It is generally accepted that IF2 and eIF5B facilitate ribosomal subunit joining during initiation[1,2,19,40]. However, a particular steric problem during the association of the 48S initiation complex with the 60S subunit is caused by the initiator tRNA, which is already bound to the 40S P site and has to find its way into the 60S P site. The direct path is blocked because the opening between the central protuberance of the 60S and the rim of the peptidyl transferase cleft with helix H69 is too narrow to allow passage of the T stem and the acceptor-stem arm of the tRNA in its canonical orientation, which is roughly perpendicular to the trajectory of the tRNAs from A site to E site (**Fig. 5a**,**b**). Therefore, it is plausible that the presence of initiator tRNA on 40S impedes subunit joining. Indeed, stable canonical or IRES analogs of 48S complexes do not join 60S subunits spontaneously after eIF5-induced hydrolysis of eIF2–GTP[2,16]. By contrast, vacant 40S and 60S subunits readily form 80S complexes without eIF5B (**Supplementary Fig. 5**), even at physiological magnesium concentration. The two substates of the present 80S initiation complex delineate a trajectory of P-site tRNA during eIF5B-facilitated ribosomal subunit joining, which in turn suggests how the tRNA is wiggled into the 60S P site by a combination of intersubunit rearrangements of the ribosome and conformational changes of the initiator tRNA itself (**Fig. 5b**). Thus, the identification of two different substates of the 80S initiation complex provides critical insights into the molecular mechanism of eIF5B-promoted subunit joining and suggests a role of eIF5B as a tRNA-reorientation factor.

Model for the last step of translation initiation

In prokaryotes, single-molecule fluorescence resonance energy transfer experiments have suggested that 70S-dependent IF2–GTP hydrolysis drives rotation of the 30S from the rotated to the nonrotated state[41]. So far, 70S complexes with IF2 have been visualized in the rotated state only. However, as we have shown here, the predominant conformational mode of the 80S–HCV-IRES–Met-tRNA$_i^{Met}$–eIF5B–GMPPNP complex is not intersubunit rotation but the eukaryotic-specific 40S-subunit rolling. Thus, although the last step of translation initiation uses large-scale conformational changes of the ribosome in both domains of life, the exact molecular mechanism appears quite different. At the transition from initiation to elongation, the ribosome has to be in the Post state to allow A-site occupation as the first step of elongation. Therefore, we consider the present Pre-like state of the 80S–HCV-IRES–Met-tRNA$_i^{Met}$–eIF5B–GMPPNP complex as the state immediately after subunit joining (**Fig. 6a**) and the Post-like state as an intermediate during the transition of the Pre-like state to the elongating Post state. In this way, the Pre-like state is functionally equivalent to the rotated state in the bacterial system. This sequence of events is corroborated by the finding that eIF5B interacts with the GAC, which is important for triggering GTPase only in the Pre-like state.

Subunit reverse rolling to the Post-like state results in a more open factor-binding-site region. As eIF5B remains attached to the 40S, reverse rolling disrupts the interaction network of eIF5B domains I and III with the SRL and the GAC of the 60S (**Fig. 3a**,**b**). According to recent crystal structures of isolated eIF5B, transition from the GTP-bound to the GDP-bound state allows an interdomain rearrangement so that domain III and the G domain associate, and domain II rotates counterclockwise by approximately 30° with respect to the G domain[32]. The use of the nonhydrolyzable GTP analog GMPPNP for 80S–eIF5B complex assembly, while allowing subunit rolling, hinders domain rearrangement of eIF5B in our structures and therefore prevents the dissociation of eIF5B–GMPPNP, owing to the high affinity of the factor for the 40S subunit in the GTP state (**Supplementary Table 1** and **Supplementary Fig. 4e**,**f**)[2,12]. However, we suggest that reverse rolling followed by conformational changes in eIF5B after GTP hydrolysis (as seen for the isolated eIF5B structures) destabilizes the interactions of eIF5B domains II and III with the 40S subunit in the Post-like state (**Supplementary Table 1**) and hence may facilitate release of eIF5B–GDP from the Post-like state. The CCA end of Met-tRNA$_i^{Met}$ is not yet placed into to the classical P/P position, and it is expected to shift from the P/pa configuration (Post-like state) into the canonical P/P position upon release of eIF5B from the ribosome (**Fig. 6b**).

According to our cryo-EM maps of the 80S–HCV-IRES–Met-tRNA$_i^{Met}$–eIF5B–GMPPNP complex, domain IV of eIF5B has a direct interaction with the acceptor stem of Met-tRNA$_i^{Met}$ but has little contact with the ribosome. This may facilitate movement of domain IV relative to the 60S during rolling of the 40S subunit to guide domain IV–Met-tRNA$_i^{Met}$ from the P^I to the P/pa state. The movement and positioning of domain IV in turn is controlled by the linker helix 12, which connects domain IV to domain III. Interestingly, mutational studies indicate that the exact length and rigidity of helix 12 are dispensable for GTP hydrolysis but required for 80S-complex assembly and stability as well as proper Met-tRNA$_i^{Met}$ binding. As previously suggested by Dever and co-workers[42] and as rationalized now in our structures, helix 12 of eIF5B rigidly links the GTPase event and the arrangement of the domain IV–Met-tRNA$_i^{Met}$ position during subunit joining. It may stabilize Met-tRNA$_i^{Met}$ along its trajectory on the 80S ribosome during subunit rolling.

METHODS

Methods and any associated references are available in the online version of the paper.

Accession codes. The electron density map and model of the 80S–HCV-IRES–Met-tRNA$_i^{Met}$–eIF5B–GMPPNP complex have been deposited in the Electron Microscopy Data Bank and Protein Data Bank under accession codes EMD-2682 and PDB 4UQ5 (40S subunit), 4UPW (60S subunit rRNAs), 4UPX (60S subunit proteins) and 4UPY (eIF5B, Met-tRNAiMet, HCV-IRES) for the Pre-like state and EMD-2683 and PDB 4UQ4 (40S subunit), 4UQ0, (60S subunit rRNAs) 4UQ1, (60S subunit proteins) and 4UPZ (eIF5B, Met-tRNAiMet, HCV-IRES) for the Post-like state.

Note: Any Supplementary Information and Source Data files are available in the online version of the paper.

ACKNOWLEDGMENTS

We thank T.V. Pestova (SUNY Downstate Medical Center) for expression vectors of eIF5B$_{587–1220}$ (ΔeIF5B) and of *Escherichia coli* methionyl-tRNA synthetase, P. Lukavsky (ETH Zürich), for the HCV-IRES construct, T. Budkevich for help with tRNA purification, J. Ismer for help with modeling of the N-terminal part of eIF5B, C. Lally for proofreading of the manuscript and K. Yamamoto for helpful discussion. This work was supported by a grant from the German Research Foundation (DFG; SFB 740, Forschergruppe 1805) to C.M.T.S. A.U. acknowledges a Rahel Hirsch fellowship from the Charité Universitätsmedizin Berlin.

AUTHOR CONTRIBUTIONS

A.U. and H.Y. established the *in vitro* system for the reconstitution of initiation complexes. H.Y. prepared the 80S–HCV-IRES–Met-tRNA$_i^{Met}$–eIF5B–GMPPNP complex. H.Y., J.B. and T.M. collected cryo-EM data. H.Y., J.L., E.B. and C.M.T.S. processed images. H.Y. and E.B. did the modeling. M.C. built the model of HCV-IRES RNA. H.Y., A.U. and C.M.T.S. discussed results and wrote the paper.

COMPETING FINANCIAL INTERESTS

The authors declare no competing financial interests.

1. Aitken, C.E. & Lorsch, J.R. A mechanistic overview of translation initiation in eukaryotes. *Nat. Struct. Mol. Biol.* **19**, 568–576 (2012).
2. Pestova, T.V. *et al.* The joining of ribosomal subunits in eukaryotes requires eIF5B. *Nature* **403**, 332–335 (2000).
3. Choi, S.K., Lee, J.H., Zoll, W.L., Merrick, W.C. & Dever, T.E. Promotion of met-tRNAiMet binding to ribosomes by yIF2, a bacterial IF2 homolog in yeast. *Science* **280**, 1757–1760 (1998).
4. Wilson, S.A. *et al.* Cloning and characterization of hIF2, a human homologue of bacterial translation initiation factor 2, and its interaction with HIV-1 matrix. *Biochem. J.* **342**, 97–103 (1999).
5. Carrera, P. *et al.* VASA mediates translation through interaction with a *Drosophila* yIF2 homolog. *Mol. Cell* **5**, 181–187 (2000).
6. Strunk, B.S., Novak, M.N., Young, C.L. & Karbstein, K. A translation-like cycle is a quality control checkpoint for maturing 40S ribosome subunits. *Cell* **150**, 111–121 (2012).
7. Pestova, T.V. *et al.* Molecular mechanisms of translation initiation in eukaryotes. *Proc. Natl. Acad. Sci. USA* **98**, 7029–7036 (2001).
8. Roll-Mecak, A., Cao, C., Dever, T.E. & Burley, S.K. X-ray structures of the universal translation initiation factor IF2/eIF5B: conformational changes on GDP and GTP binding. *Cell* **103**, 781–792 (2000).
9. Unbehaun, A. *et al.* Position of eukaryotic initiation factor eIF5B on the 80S ribosome mapped by directed hydroxyl radical probing. *EMBO J.* **26**, 3109–3123 (2007).
10. Pisarev, A.V. *et al.* Specific functional interactions of nucleotides at key –3 and +4 positions flanking the initiation codon with components of the mammalian 48S translation initiation complex. *Genes Dev.* **20**, 624–636 (2006).
11. Lee, J.H., Choi, S.K., Roll-Mecak, A., Burley, S.K. & Dever, T.E. Universal conservation in translation initiation revealed by human and archaeal homologs of bacterial translation initiation factor IF2. *Proc. Natl. Acad. Sci. USA* **96**, 4342–4347 (1999).
12. Lee, J.H. *et al.* Initiation factor eIF5B catalyzes second GTP-dependent step in eukaryotic translation initiation. *Proc. Natl. Acad. Sci. USA* **99**, 16689–16694 (2002).
13. Shin, B.S. *et al.* Uncoupling of initiation factor eIF5B/IF2 GTPase and translational activities by mutations that lower ribosome affinity. *Cell* **111**, 1015–1025 (2002).
14. Pestova, T.V., de Breyne, S., Pisarev, A.V., Abaeva, I.S. & Hellen, C.U. eIF2-dependent and eIF2-independent modes of initiation on the CSFV IRES: a common role of domain II. *EMBO J.* **27**, 1060–1072 (2008).
15. Terenin, I.M., Dmitriev, S.E., Andreev, D.E. & Shatsky, I.N. Eukaryotic translation initiation machinery can operate in a bacterial-like mode without eIF2. *Nat. Struct. Mol. Biol.* **15**, 836–841 (2008).
16. Locker, N., Easton, L.E. & Lukavsky, P.J. HCV and CSFV IRES domain II mediate eIF2 release during 80S ribosome assembly. *EMBO J.* **26**, 795–805 (2007).
17. Lukavsky, P.J. Structure and function of HCV IRES domains. *Virus Res.* **139**, 166–171 (2009).
18. Pestova, T.V., Borukhov, S.I. & Hellen, C.U. Eukaryotic ribosomes require initiation factors 1 and 1A to locate initiation codons. *Nature* **394**, 854–859 (1998).
19. Allen, G.S., Zavialov, A., Gursky, R., Ehrenberg, M. & Frank, J. The cryo-EM structure of a translation initiation complex from *Escherichia coli*. *Cell* **121**, 703–712 (2005).
20. Myasnikov, A.G. *et al.* Conformational transition of initiation factor 2 from the GTP- to GDP-bound state visualized on the ribosome. *Nat. Struct. Mol. Biol.* **12**, 1145–1149 (2005).
21. Shin, B.S. *et al.* rRNA suppressor of a eukaryotic translation initiation factor 5B/initiation factor 2 mutant reveals a binding site for translational GTPases on the small ribosomal subunit. *Mol. Cell. Biol.* **29**, 808–821 (2009).
22. Fernández, I.S. *et al.* Molecular architecture of a eukaryotic translational initiation complex. *Science* **342**, 1240585 (2013).
23. Loerke, J., Giesebrecht, J. & Spahn, C.M. Multiparticle cryo-EM of ribosomes. *Methods Enzymol.* **483**, 161–177 (2010).
24. Scheres, S.H. & Chen, S. Prevention of overfitting in cryo-EM structure determination. *Nat. Methods* **9**, 853–854 (2012).
25. Budkevich, T. V. *et al.* Regulation of the mammalian elongation cycle by 40S subunit rolling: a eukaryotic specific ribosome rearrangement. *Cell* **158**, 121–131 (2014).
26. Hashem, Y. *et al.* Hepatitis-C-virus-like internal ribosome entry sites displace eIF3 to gain access to the 40S subunit. *Nature* **503**, 539–543 (2013).
27. Unbehaun, A., Borukhov, S.I., Hellen, C.U. & Pestova, T.V. Release of initiation factors from 48S complexes during ribosomal subunit joining and the link between establishment of codon-anticodon base-pairing and hydrolysis of eIF2-bound GTP. *Genes Dev.* **18**, 3078–3093 (2004).
28. Budkevich, T. *et al.* Structure and dynamics of the mammalian ribosomal pretranslocation complex. *Mol. Cell* **44**, 214–224 (2011).
29. Guillon, L., Schmitt, E., Blanquet, S. & Mechulam, Y. Initiator tRNA binding by e/aIF5B, the eukaryotic/archaeal homologue of bacterial initiation factor IF2. *Biochemistry* **44**, 15594–15601 (2005).
30. Ratje, A.H. *et al.* Head swivel on the ribosome facilitates translocation by means of intra-subunit tRNA hybrid sites. *Nature* **468**, 713–716 (2010).
31. Spahn, C.M. *et al.* Domain movements of elongation factor eEF2 and the eukaryotic 80S ribosome facilitate tRNA translocation. *EMBO J.* **23**, 1008–1019 (2004).
32. Kuhle, B. & Ficner, R. eIF5B employs a novel domain release mechanism to catalyze ribosomal subunit joining. *EMBO J.* **33**, 1177–1191 (2014).
33. Spahn, C.M.T. *et al.* Hepatitis C virus IRES RNA-induced changes in the conformation of the 40S ribosomal subunit. *Science* **291**, 1959–1962 (2001).
34. Filbin, M.E., Vollmar, B.S., Shi, D., Gonen, T. & Kieft, J.S. HCV IRES manipulates the ribosome to promote the switch from translation initiation to elongation. *Nat. Struct. Mol. Biol.* **20**, 150–158 (2013).
35. Sprang, S.R. G protein mechanisms: insights from structural analysis. *Annu. Rev. Biochem.* **66**, 639–678 (1997).
36. Voorhees, R.M. & Ramakrishnan, V. Structural basis of the translational elongation cycle. *Annu. Rev. Biochem.* **82**, 203–236 (2013).
37. Connell, S.R. *et al.* Structural basis for interaction of the ribosome with the switch regions of GTP-bound elongation factors. *Mol. Cell* **25**, 751–764 (2007).
38. Villa, E. *et al.* Ribosome-induced changes in elongation factor Tu conformation control GTP hydrolysis. *Proc. Natl. Acad. Sci. USA* **106**, 1063–1068 (2009).
39. Hiraishi, H. *et al.* Interaction between 25S rRNA A loop and eukaryotic translation initiation factor 5B promotes subunit joining and ensures stringent AUG selection. *Mol. Cell. Biol.* **33**, 3540–3548 (2013).
40. Acker, M.G. *et al.* Kinetic analysis of late steps of eukaryotic translation initiation. *J. Mol. Biol.* **385**, 491–506 (2009).
41. Marshall, R.A., Aitken, C.E. & Puglisi, J.D. GTP hydrolysis by IF2 guides progression of the ribosome into elongation. *Mol. Cell* **35**, 37–47 (2009).
42. Shin, B.S. *et al.* Structural integrity of α-helix H12 in translation initiation factor eIF5B is critical for 80S complex stability. *RNA* **17**, 687–696 (2011).
43. Lomakin, I.B. & Steitz, T.A. The initiation of mammalian protein synthesis and mRNA scanning mechanism. *Nature* **500**, 307–311 (2013).

ONLINE METHODS

Purification of components for *in vitro* assembly of ribosomal complexes. Purification of ribosomal 40S and 60S subunits, eIF3, native full-length eIF5B and eIF5B$_{587–1220}$ (ΔeIF5B) from rabbit reticulocyte lysate (RRL) were performed according to published protocols[2,9]. Total native tRNA was extracted from RRL and subjected to *in vitro* aminoacylation and final purification as previously described[9,44]. An EcoRI-linearized plasmid containing the wild-type HCV-IRES (1–341) and 85 nucleotides of HCV coding sequence[16] was used for *in vitro* transcription of HCV-IRES RNA; this was followed by phenol extraction and gel filtration.

Reconstitution and purification of 80S–HCV-IRES–eIF5B–GMPPNP complexes. The mammalian 80S–Met-tRNA$_i^{Met}$–eIF5B–GMPPNP complex was assembled on a truncated HCV RNA of the common HCV genotype 1a comprising almost the entire 5′ UTR of HCV RNA and the first 30 nucleotides of the HCV polyprotein coding sequence, which is required for full IRES activity[16]. For subsequent affinity purification of ribosomal complexes with the biotin-streptavidin system[45], 5′-biotin–labeled DNA oligonucleotides (5′-CCCGAAGGCAGAAGTCCAAATGC-3′) (TIB MolBiol) were annealed to the HCV-IRES RNA (100 pmol) at 70 °C for 2 min in 30 µl water. The reaction was adjusted to buffer A (20 mM Tris-HCl, pH 7.6, 5 mM $MgCl_2$, 100 mM KCl, 0.2 mM spermidine, and 2 mM DTT) and allowed to cool down to room temperature. For assembly of binary 40S–HCV-IRES complexes, the HCV-IRES RNA–DNA-oligo hybrid (100 pmol) was incubated with 40S (50 pmol) at 37 °C for 5 min in buffer A (50 µl). To obtain 48S-like HCV-IRES complexes, the reaction was further incubated at 37 °C for 10 min with Met-tRNA$_i^{Met}$ (75 pmol), eIF5B (150 pmol), and eIF3 (200 pmol) in buffer A (1 ml), supplemented with GMPPNP (final concentration 0.4 mM). To form 80S complexes, 60S subunits (75 pmol) were added to the 48S mixture, and the incubation continued for 10 min at 37 °C.

Finally, streptavidin-Sepharose beads (GE Healthcare) were added to the 80S mixture, and bound complexes were collected by gentle centrifugation and washed with buffer A. Affinity-bound HCV-IRES–80S complexes were eluted from the resin in buffer A containing 0.4 units/µl RNase H (TaKaRa Bio).

Grid preparation, cryo-EM and image processing. The complex was diluted and flash frozen in liquid ethane on carbon-coated Quantifoil grids with a Vitrobot (FEI) device. Digital micrographs were automatically collected on a Tecnai G2 Polara (FEI) at 300 kV equipped with a F416 CMOS camera (TVIPS) with Leginon[46]. Data were collected at a defocus range between –2 to –4.5 µm and at a nominal magnification of ×115,000, resulting in a pixel size of 0.79 Å. Defocus values were determined with CTFfind3 (ref. 47). Particle images were preselected with Signature[48] and screened automatically. A total of 541,570 particle images were subjected to multiparticle refinement in SPIDER[23,30,49,50]. A previous cryo-EM map of a vacant 80S ribosome from rabbit was used as template. 182,925 particle images (33%) corresponding to the fully formed complex were isolated. The remaining particle images were split into structures corresponding to a rolled and an unrolled state, albeit with low density for tRNAs, HCV-IRES and eIF5B, during further refinement. We applied focused reassignment[28,50] followed by standard multiparticle refinement to separate two subpopulations containing strong eIF5B, Met-tRNA$_i^{Met}$ and HCV-IRES density (**Supplementary Fig. 1**). Focused reassignment is a version of multiparticle refinement, in which binary 2D projections of a generous 3D mask are used to focus template matching to the region of high variability, for example, the space occupied by ligands in a substochiometric manner. Orientation parameters are not changed during this step, and only class membership is refined to avoid misalignment of particle images.

Both subpopulations (substate I, 34,388 particle images and substate II, 24,777 particle images) were isolated and refined individually at pixel size of 2.37 Å, with SPIDER and SPARX[51,52]. The reconstructions of substates I and II reached resolutions of 8.9 Å and 9.5 Å, respectively, according to the Fourier shell correlation with a 0.5 cutoff. For gold-standard resolution assessment, the final reconstructions were perturbed by application of a phase-randomizing filter beyond a resolution of 10 Å and a low-pass filter beyond a resolution of 15 Å to generate two intermediate-resolution references per substate. Additionally, the Eulerian angles for all particles were randomized within a 4° range. Both sets were split, and the subsets were refined independently for several rounds with SPIDER, with the randomized structures as starting references. The final resolution between these independent subsets was 8.2 Å and 8.6 Å, respectively, with a 0.143 cutoff.

Modeling of P^I-tRNA, IRES domain II of HCV-IRES mRNA, eIF5B and the uL1 stalk. The model P-tRNA structure[25] was fit as a rigid body into the tRNA-shaped density in the P^I position in the Pre-like state. The anticodon stem and D and T loops of the model P-tRNA structure agreed well with the corresponding densities, although the acceptor stem and CCA end did not (**Supplementary Fig. 3**), and their positions were verified manually. Guided by the observed density, the base-pairing at nucleotides 4 and 69 was broken, and the position of tRNA bases 1–6 and 69–73 were adjusted into the density with Coot and RCrane[53,54]. The CCA end of tRNA at 73–76 (ACCA) was substituted from P-tRNA (PDB 2J00)[55] and was adjusted into the observed density. CNS1.2 with the STAK add-on was applied for energy minimization[56,57].

The model HCV-IRES structure (nucleotides 44–351) (M.C., H.Y. and C.M.T.S., unpublished data) was subjected to rigid-body fitting into the corresponding density of the Pre-like state. HCV-IRES domain II between nucleotides 66 and 101 was branching off the observed density (**Fig. 3a**) and was modified and reconnected to it with Coot and RCrane[53,54]. The model HCV-IRES mRNA structure (domain IV, nucleotides 332 to 353) was fit into the corresponding density and reconnected. The 33 amino acids D808–T840 of the N terminus of rabbit eIF5B adjacent to the G domain were predicted to contain one α-helical structure with PSIPreD[58]. Rabbit eIF5B (D808–I1433) was generated with SWISS-MODEL[59], and separated eIF5B domains fit as rigid bodies into the observed eIF5B density and with GMPPNP from aIF5B (PDB 1G7T)[8]. Domains were reconnected with Coot[53]. The uL1 stalk (Helix 78 and uL1) from the 60S model (PDB 4CXE)[25] did not fit into the corresponding density of the Pre-like state. RNA positions 3915 to 4035 with the bound uL1 were cut off the 28S rRNA and adjusted into the observed density.

Subunit joining assay of vacant ribosomes. For 80S-complex assembly with vacant ribosomal subunits (**Supplementary Fig. 5**), 25 pmol of 40S and 60S were incubated with 75 pmol ΔeIF5B in a 120-µl reaction in buffer A1 (20 mM Tris, pH 7.5, 100 mM potassium acetate, 2 mM DTT, and 0.25 mM spermidine) and 2.5 or 5 mM $MgCl_2$ with 0.4 mM GMPPNP or GTP, or without ΔeIF5B, as indicated. The mixture was incubated for 15 min at 37 °C and loaded onto a linear 10–30% sucrose gradient (prepared in the corresponding buffer) and centrifuged for 95 min at 50,000 r.p.m. in a SW55 rotor. Gradient fractions were subjected to continuous recording of OD at 260 nm and were collected automatically with LKB equipment. Recombinant ΔeIF5B lacking the N terminus was used in this experiment and has been shown to be equally active as the full-length protein in subunit joining[2].

44. Budkevich, T.V., El'skaya, A.V. & Nierhaus, K.H. Features of 80S mammalian ribosome and its subunits. *Nucleic Acids Res.* **36**, 4736–4744 (2008).
45. Namy, O., Moran, S.J., Stuart, D.I., Gilbert, R.J. & Brierley, I. A mechanical explanation of RNA pseudoknot function in programmed ribosomal frameshifting. *Nature* **441**, 244–247 (2006).
46. Suloway, C. *et al.* Automated molecular microscopy: the new Leginon system. *J. Struct. Biol.* **151**, 41–60 (2005).
47. Mindell, J.A. & Grigorieff, N. Accurate determination of local defocus and specimen tilt in electron microscopy. *J. Struct. Biol.* **142**, 334–347 (2003).
48. Chen, J.Z. & Grigorieff, N. SIGNATURE: A single-particle selection system for molecular electron microscopy. *J. Struct. Biol.* **157**, 168–173 (2007).
49. Frank, J. *et al.* SPIDER and WEB: processing and visualization of images in 3D electron microscopy and related fields. *J. Struct. Biol.* **116**, 190–199 (1996).
50. Penczek, P.A., Frank, J. & Spahn, C.M. A method of focused classification, based on the bootstrap 3D variance analysis, and its application to EF-G-dependent translocation. *J. Struct. Biol.* **154**, 184–194 (2006).
51. Hohn, M. *et al.* SPARX, a new environment for cryo-EM image processing. *J. Struct. Biol.* **157**, 47–55 (2007).
52. Yang, Z. & Penczek, P.A. Cryo-EM image alignment based on nonuniform fast Fourier transform. *Ultramicroscopy* **108**, 959–969 (2008).
53. Emsley, P., Lohkamp, B., Scott, W.G. & Cowtan, K. Features and development of Coot. *Acta Crystallogr. D Biol. Crystallogr.* **66**, 486–501 (2010).
54. Keating, K.S. & Pyle, A.M. RCrane: semi-automated RNA model building. *Acta Crystallogr. D Biol. Crystallogr.* **68**, 985–995 (2012).

doi:10.1038/nsmb.2859

55. Selmer, M. *et al.* Structure of the 70S ribosome complexed with mRNA and tRNA. *Science* **313**, 1935–1942 (2006).
56. Brunger, A.T. Version 1.2 of the Crystallography and NMR system. *Nat. Protoc.* **2**, 2728–2733 (2007).
57. Laurberg, M. *et al.* Structural basis for translation termination on the 70S ribosome. *Nature* **454**, 852–857 (2008).
58. Buchan, D.W., Minneci, F., Nugent, T.C., Bryson, K. & Jones, D.T. Scalable web services for the PSIPRED Protein Analysis Workbench. *Nucleic Acids Res.* **41**, W349–W357 (2013).
59. Arnold, K., Bordoli, L., Kopp, J. & Schwede, T. The SWISS-MODEL workspace: a web-based environment for protein structure homology modelling. *Bioinformatics* **22**, 195–201 (2006).